Korean J. Chem. Eng., 32(7), 1273-1277 (2015)
DOI: 10.1007/s11814-014-0321-y

pISSN: 0256-1115
eISSN: 1975-7220

Homogeneous catalytic activity of gold nanoparticles synthesized using turnip (*Brassica rapa* L.) leaf extract in the reductive degradation of cationic azo dye

Kannan Badri Narayanan and Hyun Ho Park†

School of Biotechnology and Graduate School of Biochemistry, Yeungnam University, Gyeongsan 712–749, Korea
(*Received 17 June 2014 • accepted 29 October 2014*)

Abstract−A new greener strategy for the synthesis and stabilization of gold nanoparticles using aqueous turnip leaf extract under ambient conditions is reported in this study. The formation of gold nanoparticles was monitored using a UV-Vis spectrophotometer and the maximum absorption peak (λ_{max}) at 535 nm with a visual color change to pinkish-red confirmed the gold nanoparticles. Further characterization was conducted using Fourier-transform Infra-red spectrometry (FT-IR), powder X-ray diffractometry (XRD), transmission electron microscopy (TEM), and dynamic light scattering (DLS) with zeta potential at pH 7.5. The stability of the nanoparticles was due to the capping of nanoparticles with amine groups and ortho-substituted aromatic phytoconstituents, which exhibit higher negative values of zeta potential (ζ). XRD pattern revealed the formation of face-centered cubic (fcc) lattice crystals of gold nanoparticles, while TEM have demonstrated the size of gold nanoparticles ranging from 3 to 58 nm. The as-synthesized gold nanoparticles showed rapid catalytic reduction of methylene blue (MB) dye to leuco MB in the presence of sodium borohydride ($NaBH_4$). The reduction reaction followed pseudo-first order kinetics with a reaction rate constant of 0.372 min^{-1}. This process of nanoparticle synthesis is simple, nontoxic and environmentally benign compared to the chemical synthetic routes.

Keywords: Gold Nanoparticles, Electron Microscopy, Turnip Leaf, Catalyst, Pseudo-first Order Kinetics, Methylene Blue Dye

INTRODUCTION

Metal nanoparticles are effective catalysts for various organic reactions because of their high efficiency under environmentally benign reaction conditions. The surface-to-volume ratio of nanoparticles provides increased active sites for a high rate of chemical reaction. In particular, gold nanoparticles act as catalysts in terms of selectivity, reactivity and improved yields of products, and the catalytic activity of gold nanoparticles has been documented in several hydrogenation and oxidation reactions [1]. The synthesis of advanced nanomaterials using several biomimetic methodologies inspired from natural processes has recently been rapidly expanding, and the synthesis of metal nanoparticles (MNPs) such as gold, silver, copper, platinum, and palladium with specific shapes and sizes for its unique applications has been accomplished. Additionally, microorganisms, microbial extracts, plants and plant extracts have been widely used to synthesize MNPs using a green chemistry approach [2]. The readily available sustainable materials are particularly focused on the synthesis of MNPs; therefore, the use of plant extracts deserves attention owing to its rapidity, cost-effectiveness, easy scalability, reliability and non-toxicity. Accordingly, investigation of a wide variety of plants for the ability to bioreduce metals has increased.

Several natural compounds present in plant extracts have been shown to be agents for the synthesis of MNPs. The leaf extracts of lemon grass [3], neem [4], Indian gooseberry [5], tamarind [6], aloe vera [7], camphor tree [8], coriander and *Coleus amboinicus* [2], tea plant [9], henna [10], *Phyllanthusamarus* [11], guava [12], *Magnolia kobus* and Persimmon [13], *Ocimum sanctum* [14], *Cissusquadrangularis* [15], and *Cynodondactylon* [16] have been shown to synthesize gold and silver nanoparticles with unique sizes and shapes. *Brassica rapa* L. belongs to the *Brassicaceae* family, which contains abundant phenolic compounds that, depending on their structure, can be classified into simple phenols, phenolic acids, hydroxycinnamic acid and flavonoids. Many of these compounds possess antioxidant properties [17]. Methylene blue (MB) is a heterocyclic aromatic compound as well as cationic azo dye with the molecular formula $C_{16}H_{18}N_3SCl$ that has been applied intravenously at doses of 1-7.5 mg/kg for the treatment of methemoglobinemia and vasoplegia, and as an aid in parathyroidectomy. However, MB was recently found to cause severe central nervous system (CNS) toxicity [18], and it has also been reported to be mutagenic toward *Salmonella typhimurium* under visible light strains [19]. MB in aqueous solution produces a blue color, which is reduced to colorless leuco MB (LMB). LMB can be further oxidized (red-ox ability), resulting in its having applications in sensors, data storage devices, electro-optic devices, oxygen detectors and time duration monitoring and the textile industry [20]. Edison and Sethuraman [21] used a green chemistry process for the synthesis of silver nanoparticles, which were subsequently used as catalysts for the reduction of azo-dye, methylene blue. Herein, we report the synthesis of gold nanoparticles using aqueous turnip leaf extract and the ability of the synthesized particles to catalyze the reduction of the cationic

†To whom correspondence should be addressed.
E-mail: hyunho@ynu.ac.kr

azo dye methylene blue, which is a common contaminant of aqueous effluents from the textile industry.

MATERIALS AND METHODS

1. Materials

All reagents purchased were of analytical grade. Chloroauric acid ($HAuCl_4$) was purchased from Alfa Aesar (China), while sodium borohydride ($NaBH_4$) and methylene blue were purchased from Junsei Chemical Co. Ltd. (Tokyo, Japan). Turnip leaves (*Brassica rapa* L.) were purchased from Gyeongsan market, South Korea. All aqueous solutions were prepared using double distilled water and all experiments were conducted in triplicate.

2. Synthesis of Gold Nanoparticles by Turnip Leaves

Briefly, 30 g of turnip leaves was collected and thoroughly washed in sterile distilled water, after which they were chopped into small pieces, added to 100 ml of deionized sterile water and heated at 90 °C for 30 min in a water bath. The solution was then filtered and stored at 4 °C as stock solution for experiments. For the reduction of gold ions, 1 ml of leaf extract was added to 5 ml of 1 mM $HAuCl_4$ and then incubated at 70 °C. The synthesis of gold nanoparticles was monitored by visual inspection and further characterized.

3. Characterization of Gold Nanoparticles

The resultant gold colloids were visually monitored through color change, while UV-Vis absorbance between 200 and 1,000 nm was periodically measured with a UV-Vis spectrophotometer (Beckman Coulter DU-730). To investigate the particle size, size distribution and zeta potential (ζ), the particles were characterized by dynamic light scattering (DLS) using a Malvern Zetasizer Nano (Malvern Instruments Ltd., UK). All measurements were conducted in triplicate using automated, optimal measurement time and laser attenuation settings at 25 °C. The size and morphology of gold nanoparticles were determined by transmission electron microscopic (TEM) images. Samples were deposited on lacey carbon-coated copper 200 mesh grids and allowed to dry in air prior to measurements on a TEM (Hitachi; Model H7600) microscope operated at an accelerating voltage of 120 kV. Powder X-ray diffraction (XRD) of colloidal gold nanoparticles was performed on a PANalytical X'pert PRO X-ray diffractometer (Netherlands) at a voltage of 40 kV and a current of 30 mA with CuKα1 radiation (1.541 Å) [22]. For FTIR analysis, gold colloid solution was centrifuged at 25,000 ×*g* for 20 min and the pellet was then washed in sterile double distilled water. This process was conducted three times to remove all unbound proteins and other residues. The purified nanoparticle sample was then dried and ground with KBr powder, after which it was pelleted for subsequent analysis on a Jasco FTIR 5300 spectrophotometer.

4. Catalytic Activity of Gold Nanoparticles in the Reduction of Methylene Blue

The reduction of methylene blue (MB) by sodium borohydride ($NaBH_4$) in the presence of biologically synthesized gold nanoparticles as a homogeneous catalyst at 25 °C was conducted. To achieve final concentrations of 5×10^{-5} M (MB) and 3.3×10^{-3} M ($NaBH_4$), 5.77 ml of distilled water was added to 30 µl of 0.01 M MB and then mixed with 200 µl of freshly prepared 0.1 M $NaBH_4$ and agitated in the presence of gold colloid for the reduction reaction. The rate constant of the reduction of MB was calculated by measuring the change in methylene blue absorbance at 664 nm with respect to time. The reference reaction unsupported by gold nanocatalyst was also monitored at different time intervals using a UV-Vis spectrophotometer.

RESULTS AND DISCUSSION

1. Characterization of Gold Nanoparticles

Gold in the bulk state is chemically inert, but becomes chemically reactive at the nanoscale. Specifically, gold nanoparticles exhibit surface plasmon resonance (SPR) with pinkish-red color in aqueous solution [23]. The green synthesis of gold nanoparticles using non-toxic chemicals as reducing and stabilizing agents is one of the best environmentally-benign approaches currently available. Conventional methodologies use chemicals such as hydrazine, $NaBH_4$, and ascorbic acid, which form free radicals for the reduction of Au^{3+} to Au^0 and some polysaccharides such as starch and proteins to

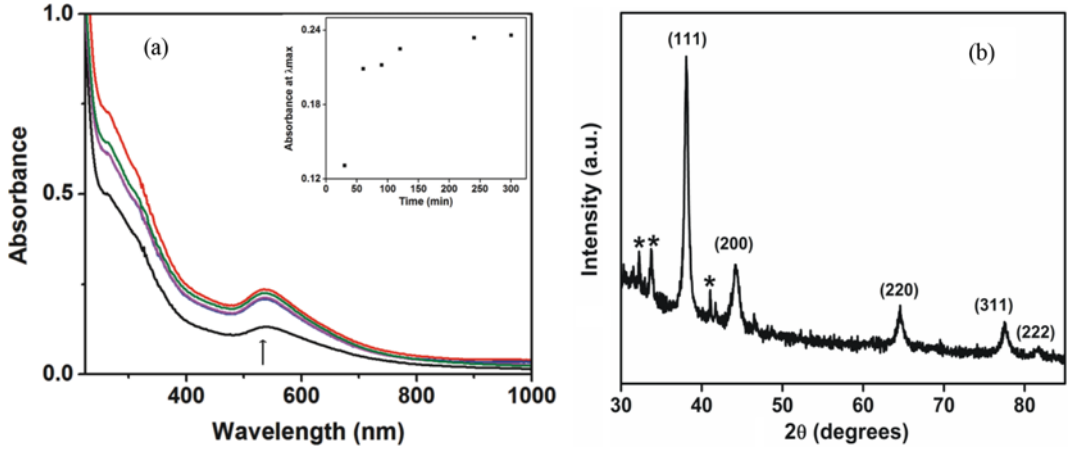

Fig. 1. (a) UV-vis spectra of gold colloid synthesized at different reaction times using aqueous turnip leaf extract at 70 °C. The insert is a plot of maximum absorbance (λ_{max}) vs. time of reaction of gold chloride solution. (b) XRD pattern of gold nanoparticles synthesized using aqueous turnip leaf extract at 70 °C. The unassigned peaks (*) correspond to the bio-organic phase of leaf extract.

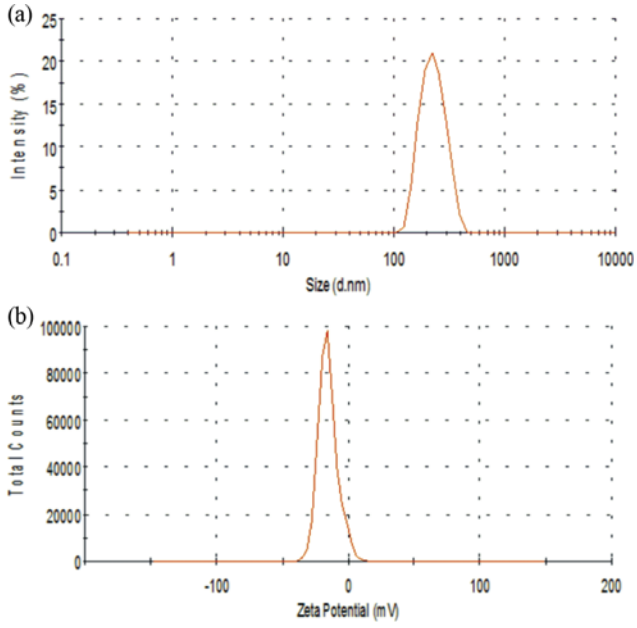

Fig. 2. (a) DLS and (b) zeta potential of gold colloid in water phase.

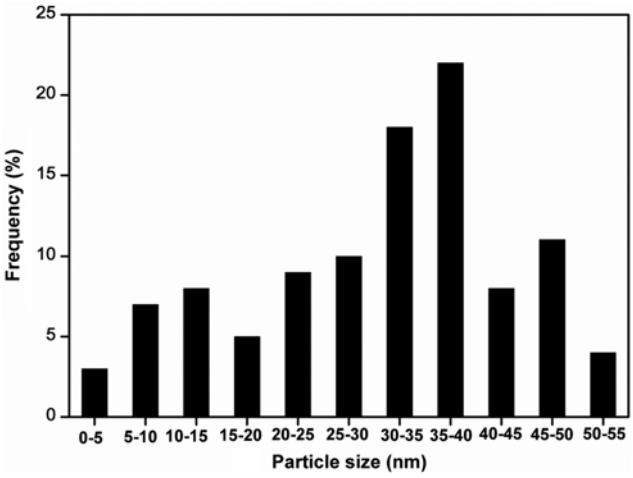

Fig. 4. Histogram of percent frequency distribution of gold nanoparticles.

stabilize the nanoparticles. However, turnip leaves extract containing several sugars, metabolites and peptides are all involved in the reduction and stabilization of gold nanoparticles for better dispersity and morphology. The formation of metal nanoparticles can be ascertained by measuring the UV-Vis absorption spectra. The absorption peak at 535 nm is due to the SPR band of gold nanoparticles. The shape and position of the absorbance band preview the morphology of nanoparticles. The symmetric SPR peak indicates the formation of predominant isotropic spherical nanoparticles, while a slightly broadened tail indicates little aggregation (Fig. 1(a)). The physico-chemical properties of nanoparticles are dependent on their size and shape. DLS measurements revealed the hydrodynamic size of the gold nanoparticles. Specifically, a single major peak at ca. 230 nm was observed, indicating an average diameter with polydispersity index (pdI) of 0.213 and a zeta potential of −15.3 at pH 7.5 (Fig. 2). The exact size and morphology of the nanoparticles were imaged using transmission electron microscopy (TEM). TEM results revealed the formation of spherical nanoparticles ranging from 3 to 58 nm in size with an average size of 31.4±14.9 nm at a magnification of ×20k and ×100k (Fig. 3 and 4). Powder XRD pattern revealed the crystallinity of synthesized gold nanoparticles. The diffraction peaks were observed at 2θ values of 38.08, 44.16, 64.57, 77.62 and 81.8 corresponding to Bragg's reflections of (111), (200), (220), (311) and (222) planes for the face-centered-cubic (fcc) structure of gold nanoparticles (JCPDS No. 002-1095). The presence of unassigned peaks indicates the formation of a bio-organic phase from the leaf extract (Fig. 1(b)). FTIR spectra were used to investigate the interaction of biomolecules with gold during the formation of gold nanoparticles. The extract showed bands at 3,600-3,500 cm^{-1}, which corresponded to -NH stretching of amines. The bands at 2,369 and 1,173 cm^{-1} corresponded to the presence of CN and C-O stretching of aliphatic esters, respectively. Upon interaction with metals, the intensity of these bands decreased considerably with changes in the transmission region. Most of the amines are good ligands for metal ions to form coordination complexes, specifically, the band in the 3,396 cm^{-1} region shifted to a higher frequency due to the bonds of gold with nitrogen atoms [24], while the band at 1,588 cm^{-1} corresponded to ortho-substituted aromatic compounds, and the band at 2,862 cm^{-1} corresponded to -CH stretching in $-CH_3$ attached to O or N (Fig. 5). Zakaria et al. [25] demonstrated the stabilization of colloidal gold in the presence of anionic carboxyl groups, while Selvakannan et al. [26] demonstrated that silver ions reduction at high pH occurs due to ionization of the phenolic group in tyrosine, which can reduce Ag^{+} ions, which are then

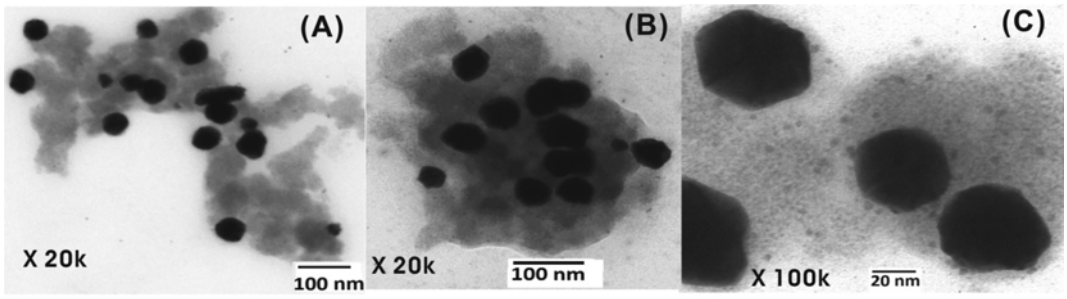

Fig. 3. TEM images of gold nanoparticles at different magnifications of ((A), (B)) ×20k and (C) ×100k.

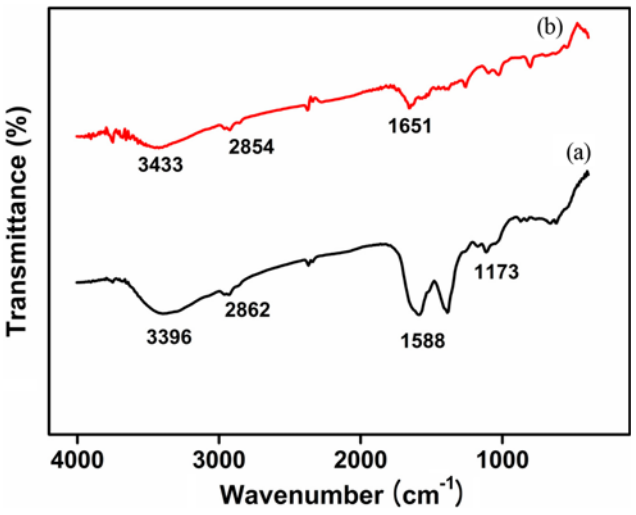

Fig. 5. FT-IR spectra of (a) turnip leaf extract and (b) gold nanoparticles synthesized after reacting with turnip leaf extract.

converted to a semi-quinone structure.

2. Catalytic Activity of Gold Nanoparticles in the Reduction of Methylene Blue

Methylene blue (MB) is a water-soluble cationic dye used as a redox indicator [27]. In aqueous oxidizing environments, MB absorbs light at around 664 nm, resulting in bright blue color. This absorption peak at 664 nm decreases smoothly and become colorless in the presence of excess of reducing agent, $NaBH_4$ [20]. Thus, the reduction forms leucomethylene blue (LMB). The absorption of MB at 664 nm is due to the n– π^* transition and another shoulder peak at 614 nm [28]. Although the reduction of MB to LMB occurs in the presence of reducing agent, the reduction rate is very slow. $NaBH_4$ is a weak reducing agent used in many industrial processes as well as in wastewater treatment that generates hydrogen gas via a hydrolysis reaction in aqueous solution. The catalytic activity of gold nanoparticles at the nanoscale is due to the reduction of its redox potential to a negative value [29,30]. Thus, gold nanoparticles facilitate the transfer of electrons (e^-) from BH_4^- ions to MB in the catalytic reduction process of MB to LMB [31]. Mahmoodi [32] demonstrated the dye removal ability of amine-functionalized magnetic ferrite nanoparticle. Saatci [33] decolorized and mineralized azo-reactive textile dye, Remazol Red F3B by Fenton and photo-Fenton processes.

The reduction of MB as a function of time in the presence of $NaBH_4$ and gold nanoparticles was also investigated. Upon addition of $NaBH_4$ as a reducing agent in the presence of gold nanoparticles as a catalyst, the intensity of absorbance at 664 nm by MB decreases rapidly with the time, confirming that gold nanoparticles act as an effective catalyst during the rapid reduction of MB. The reduction of MB in the presence and absence of gold nanoparticles was monitored for 20 min. In the presence of gold nanoparticles, there was a steady decrease in the absorbance peak (λ_{max}) with no change in the shape and position of the absorption band, which indicates that MB is reduced without any other chemical reactions (Fig. 6(a)). In reactions without the addition of gold nanoparticles, the reduction rate was very slow.

The order of the reduction reaction follows pseudo-first order kinetics since the concentration of BH_4^- is higher than that of MB and remains constant throughout the reaction (i.e. the rate of reduction of MB is independent of the concentration of $NaBH_4$). The reaction kinetics showed a good linear correlation between ln(A) and reaction time [34], and the rate constant was estimated to be 0.372 min^{-1} for gold nanoparticles of ca. 25 nm (Fig. 6(b)). Cheval et al. [28] demonstrated catalytic reduction of methylene blue dye using polyamide 66 microspheres metallized with *in situ* synthesized gold nanoparticles. Srivastava et al. [35] showed the catalytic reduction of 4-nitrophenol using biogenic gold nanoparticles. Similarly, Panigrahi et al. [36] demonstrated the reduction of 4-nitrophenol to 4-aminophenol using resin supported gold nanoparticles.

CONCLUSIONS

This study demonstrated that turnip leaf extract can be used as a non-toxic, sustainable, renewable organic source for the synthesis of gold nanoparticles of varying size and shape. Phytochemicals containing amine groups and ortho-substituted aromatic com-

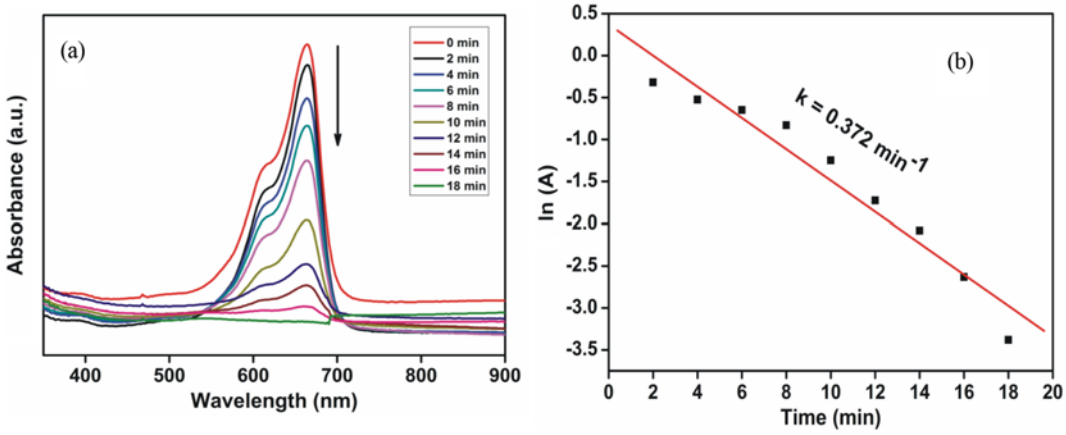

Fig. 6. (a) UV-vis absorbance spectra for the reduction of methylene blue using $NaBH_4$ supported by gold nanoparticles. (b) Plot of ln(A) against time for the catalytic reduction of methylene blue by gold nanoparticles.

pounds act as capping agents in the stabilization of nanoparticles. XRD revealed that the as-synthesized gold nanoparticles were crystalline with fcc geometry, while TEM images revealed that the particles were ca. 45 nm. These gold nanoparticles are effective catalysts in the reduction of methylene blue using $NaBH_4$ through electron relay effect in a reduction reaction that follows pseudo-first order kinetics.

ACKNOWLEDGEMENT

This research was supported by a grant from the Korea Healthcare Technology R&D Project, Ministry of Health and Welfare, Republic of Korea (HI13C1449).

REFERENCES

1. Z. Ma, S. H. Overbury and S. Dai, *Gold nanoparticles as chemical catalysts*, Encyclopedia of Inorganic Chemistry (2009).
2. K. B. Narayanan and N. Sakthivel, *Adv. Colloid Interface Sci.*, **169**, 59 (2011).
3. S. S. Shankar, A. Rai, B. Ankamwar, A. Singh, A. Ahmad and M. Sastry, *Nat. Mater.*, **3**, 482 (2004).
4. S. S. Shankar, A. Rai, A. Ahmad and M. Sastry, *J. Colloid Interface Sci.*, **275**, 496 (2004).
5. B. Ankamwar, C. Damle, A. Ahmad and M. Sastry, *J. Nanosci. Nanotechnol.*, **5**, 1665 (2005).
6. B. Ankamwar, M. Chaudhary and M. Sastry, *Synth. React. Inorg. Met-Org. Nanometal Chem.*, **35**, 19 (2005).
7. S. P. Chandran, M. Chaudhary, R. Pasricha, A. Ahmad and M. Sastry, *Biotechnol. Prog.*, **22**, 577 (2006).
8. J. Huang, Q. Li, D. Sun, Y. Lu, Y. Su, X. Yang, H. Wang, Y. Wang, W. Shao, N. He, J. Hong and C. Chen, *Nanotechnology*, **18**, 105104 (2007).
9. R. Vilchis-Nestor, V. Sanchez-Mendieta, M. A. Camacho-Lopez, R. M. Gomez-Espinosa, M. A. Camacho-Lopez and J. A. Arenas-Alatorre, *Mater. Lett.*, **62**, 3103 (2008).
10. J. Kasthuri, S. Veerapandian and N. Rajendiran, *Colloids Surf., B Biointerfaces*, **68**, 55 (2009).
11. J. Kasthuri, K. Kathiravan and N. Rajendiran, *J. Nanopart. Res.*, **11**, 1075 (2009).
12. D. Raghunandan, S. Basavaraja, B. Mahesh, S. Balaji, S. Y. Manjunath and A. Venkataraman, *Nanobiotechnology*, **5**, 34 (2009).
13. J. Y. Song, H. K. Jang and B. S. Kim, *Process Biochem.*, **44**, 1133 (2009).
14. G. Singhal, R. Bhavesh, K. Kasariya, A. R. Sharma and R. P. Singh, *J. Nanopart. Res.*, **13**, 2981 (2011).
15. J. S. Valli and B. Vaseeharan, *Mater. Lett.*, **82**, 171 (2012).
16. N. Sahu, D. Soni, B. Chandrashekhar, B. K. Sarangi, D. Satpute and R. A. Pandey, *Bioproc. Biosyst. Eng.*, **36**, 999 (2013).
17. M. E. Cartea, M. Francisco, P. Soengas and P. Velasco, *Molecules*, **16**, 251 (2011).
18. P. K. Gillman, *J. Psychopharmacol.*, **25**, 429 (2011).
19. B. Epe, J. Hegler and D. Wild, *Carcinogenesis*, **10**, 2019 (1989).
20. Y. Galagan and W. F. Su, *J. Photochem. Photobiol.*, **195**, 378 (2008).
21. T. J. I. Edison and M. G. Sethuraman, *Process Biochem.*, **47**, 1351 (2012).
22. P. Klug and L. E. Alexander, *X-ray diffraction procedures for polycrystalline and amorphous materials*, 2nd Ed., Wiley, New York (1974).
23. B. Hvolbaek, T. V. W. Janssens, B. S. Clausen, H. Falsig, C. H. Christensen and J. K. Norshov, *Nano Today*, **2**, 14 (2007).
24. M. Valodkar, R. N. Jadeja, M. C. Thounaojam, R. V. Devkar and S. Thakore, *Mater. Chem. Phys.*, **128**, 83 (2011).
25. H. M. Zakaria, A. Shah, M. Konieczny, J. A. Hoffmann, A. J. Nijdam and M. E. Reeves, *Langmuir*, **29**, 7661 (2013).
26. P. R. Selvakannan, A. Swami, D. Srisathiyanarayanan, S. Shirude, R. Pasricha, A. Mandale and M. Sastry, *Langmuir*, **20**, 7825 (2004).
27. N. I. Surovtseva, A. M. Eremenko, N. P. Smirnova, V. A. Pokrovskii, T. V. Fesenko and G. N. Starukh, *Theor. Exp. Chem.*, **43**, 235 (2007).
28. N. Cheval, N. Gindy, C. Flowkes and A. Fahmi, *Nanoscale Res. Lett.*, **7**, 182 (2012).
29. M. Haruta, *J. Catal.*, **115**, 301 (1989).
30. I. Laoufi, R. Lazzari, J. Jupille, O. Robach, S. Garaud, G. Cabailh, P. Dolle, H. Cruguel and A. Bailly, *J. Phys. Chem. C*, **115**, 4673 (2011).
31. K. B. Narayanan and N. Sakthivel, *Bioresour. Technol.*, **102**, 10737 (2011).
32. N. M. Mahmoodi, *J. Environ. Eng.*, **139**, 1382 (2013).
33. Y. Saatci, *J. Environ. Eng.*, **136**, 1000 (2010).
34. K. B. Narayanan and N. Sakthivel, *J. Hazard. Mater.*, **189**, 519 (2011).
35. S. K. Srivastava, R. Yamada, C. Ogino and A. Kondo, *Nanoscale Res. Lett.*, **8**, 70 (2013).
36. S. Panigrahi, S. Basu, S. Praharaj, S. Pande, S. Jana, A. Pal, S. K. Ghosh and T. Pal, *J. Phys. Chem. C*, **111**, 4596 (2007).